

Article

An Ultra-Wideband Compact TR Module Based on 3-D Packaging

Zhiqiang Li ^{1,2}, Houjun Sun ^{1,*}, Hongjiang Wu ² and Shuai Zhang ²

¹ Beijing Key Laboratory of Millimeter Wave and Terahertz Techniques, School of Information and Electronics, Beijing Institute of Technology, Beijing 100081, China; 3220160014@bit.edu.cn

² China Electronics Technology Group Corporation, The 13th Research Institute, Shijiazhuang 050051, China; hesy@cetc13.cn (H.W.); zhangshuai@163.com (S.Z.)

* Correspondence: sunhoujun@bit.edu.cn

Abstract: This study presents a novel four-channel tile-type T/R module which achieves excellent performances in ultra-wideband (2–12 GHz) and integrates all circuits in a super-light (25 g) and compact ($27.8 \times 27.8 \times 12 \text{ mm}^3$) mechanical structure in active phased array systems. The key advancement of this T/R module was to choose a Ball Grid Array (BGA) as the vertical interconnection and bracing between High-Temperature Co-fired Ceramic (HTCC) substrates in order to achieve a high-integration 3-D structure. Exploiting the HTCC multilayer layout, this paper presents the design and development of an ultra-wideband, compact and light, high-output power, four-channel, dual-polarization Transmit/Receive (T/R) Module. In this module, microwave circuits and power control circuits are highly integrated into electrically isolated HTCC layers or substrates, resulting in low coupling and crosstalk between signals. Furthermore, multichip assembly technology, multifunctional MMICs, and other high-integration technologies were adopted for this module. Each channel could provide more than 2 W transmit output power, more than 15 dB receive gain, and less than 5 dB receive noise figure. Every module contains four channels. The power supply and phase/amplitude conditioning of each channel can be controlled individually and showed good consistency of the amplitude and phase of all channels. The connectors of manifold port and polarization ports are all SSMP, which can achieve further integration. This module has also an automatic negative power protection function. The module has stabilized performance and mass production prospects.

Keywords: T/R module; tile type; 3-D integrated packaging; high power; ultra-wideband; miniaturization



check for updates

Citation: Li, Z.; Sun, H.; Wu, H.; Zhang, S. An Ultra-Wideband Compact TR Module Based on 3-D Packaging. *Electronics* **2021**, *10*, 1435. <https://doi.org/10.3390/electronics10121435>

Academic Editors: Joaquin Portilla, Patrick Roblin and Jean-Christophe Nallatamby

Received: 26 April 2021

Accepted: 8 June 2021

Published: 15 June 2021

Publisher's Note: MDPI stays neutral with regard to jurisdictional claims in published maps and institutional affiliations.



Copyright: © 2021 by the authors. Licensee MDPI, Basel, Switzerland. This article is an open access article distributed under the terms and conditions of the Creative Commons Attribution (CC BY) license (<https://creativecommons.org/licenses/by/4.0/>).

1. Introduction

The active phased arrays technology is widely used in radar systems, electronic warfare, and other telecommunication applications. Active phased arrays radar systems have become the mainstream of today's radar systems for research and development [1–3]. Transmit/receive modules with outstanding performance and high reliability are one of the key elements in active phased array radar systems. All radiation channels of the T/R module are capable of signal amplification, phase/amplitude conditioning, and beam management. A T/R module basically consists of RF switches, power amplifiers, low-noise amplifiers, phase shifters, attenuators, power supply circuits, logic control circuits, and other functional circuits. All of these RF chips and circuits have covered microwave integrated circuits, high-speed digital circuits, and other technical fields. Active phased array radar systems with T/R modules will play an increasingly important role in airborne, space, missile, and other applications [4–6].

The weight, dimensions, performance, and reliability of the T/R module can directly affect the characteristics of an active phased array radar system. Therefore, as the key part of active phased array systems for airborne, missile, or other mobile platforms, the T/R module have high requirements: wide operating bandwidth, high reliability, high output

power, compactness, and light weight. Therefore, it is required to reduce the layout area while satisfying the electrical characteristics of T/R modules [7–9].

In recent years, T/R modules containing HTCC substrates have become a widespread concern worldwide. HTCC substrates are fabricated by laminating and sintering multilayer ceramic together, forming a hard and dense ceramic component with high temperature stability, high strength, and good coefficient of expansion, matching with integrated circuits. Therefore, they are easy to integrate with MMICs and suitable for high-frequency and low-frequency hybrid circuits and analog–digital integrated packaging [10,11]. Moreover, as a 3-D passive substrate, a high-density RF circuit and complicated passive circuit can be located on the HTCC substrate, and the benefits of extensive integrated circuit features can be seen. Furthermore, microwave multilayer interconnection, which is based on HTCC technology, is a perfect carrier and has become a popular technology used in compact modules and 3-D modules [12–15].

BGA balls and fuz buttons are popular for 3-D T/R module interconnections. The fuz button is elastic and thus is easily interconnected, but it requires an extra mounted structure which will increase the thickness of the module and affect miniaturization. In contrast, BGA balls do not have this inconvenience.

This paper is based on the HTCC (Al_2O_3) process with a BGA ball interconnection to design and develop a high-density system package, high-output power tile-type T/R module that is ultra-wideband, light and compact. The volume of the module with the HTCC board was 1/3 of the module with a single-layer board and the weight was 1/2 of it. As a result, this module resulted to have a significantly decreased volume and weight.

2. General Aspects and Requirements

2.1. Overview of the TR Module Design

The main goal of the design comes was to reduce the module size, weight, and channel array spacing, while achieving high performance in an ultra-wideband. Therefore HTCC, BGA interconnection, multifunctional MMICs technology were used to integrate the circuit into two sub-compact modules. The designed upper sub-module includes two-channel multifunctional MMICs and relevant RF circuits, power supply circuits, and logic control circuits. The lower sub-module consists of RF signal amplifier circuits, a drive amplifier, a limiter, a low-noise amplifier, and a dual polarization switch. The upper module sends the power, logic control signal, and RF signal to the lower module through the BGA ball.

2.2. Electrical Specification

The key electrical parameters of the module are summarized in Table 1.

Table 1. Key electrical parameters of the module.

Parameter	Measured Data
Frequency Range	2~12 GHz
Rx Gain	15~18 dB
Noise Figure	4.2~5.5 dB
Rx Input P ₋₁	≥ -20 dBm
Maximum Tx Gain	30 dB
Tx Output Power	32~34.5 dBm (CW)
VSWR	<1.8
Phase Variation Range	0~720° (6-bit)
RMS Phase Error	<6°
Attenuation Range	0~31.5 dB (6-bit)
RMS Attenuation Error	<0.5 dB
Tx Harmonic Suppression	≤ -15 dBc (in band), ≤ -25 dBc (out of band)
Switch Time (T/R)	<500 ns
System Bias	+5 V, +28 V, -40 V, -5 V
Package Technology	3-D multilayer package with BGA balls

The above parameters have considered the MMICs technique, yet it is still challenging for the HTCC multilayer routing and BGA interconnection. Another X-band tile T/R module with an LTCC package solution has a narrower bandwidth which a frequency range from 8.8 GHz to 10.4 GHz and has similar Tx output power [16]. The X-band module has one channel and dimensions of $20 \times 20 \times 2.6 \text{ mm}^3$. The module designed in this paper, however, has four channels and a similar small size.

3. Module Design

3.1. Circuit Schematic Design

In this paper, the four-channel, dual-polarization, tile-type T/R module consists of signal amplification, power control, beam management, and phase and amplitude adjustment in RF circuit. The functional block diagram of the module is shown in Figure 1.

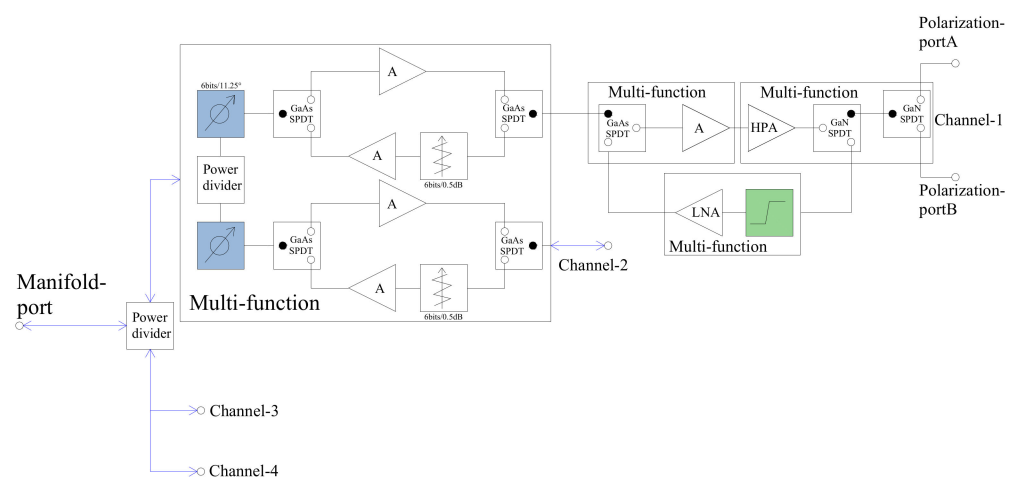


Figure 1. Tile-type functional block diagram.

Each channel is composed of branches for transmitting and receiving. The Tx/Rx modes are controlled using two Tx/Rx changeover switches. One of the switches is behind the antenna, and the other is integrated into the multifunctional IC. Polarizations are swapped using a polarization switch between the antenna and the T/R switch. To reduce the module size, a two-channel multifunctional MMIC design was used that integrates the two channels' 6-bit phase shifters, 6-bit digital attenuators, RF switch, two-way amplifier, and power divider into one single chip. The power, phase, and amplitude of the RF signal in each channel can be controlled individually, and the control circuit has an automatic negative power protection function.

If the module is in the receiving mode, the signal is first received by the antenna and then passes through the dual-polarization switch, Tx/Rx switch, limiter, low-noise amplifier, and multifunctional MMICs and is finally combined and output to the public port.

If the module is in the transmitting mode, after the excitation signal divides into two paths, each path transmits the signal through two-channel multifunctional MMICs, a drive amplifier, a power amplifier, and an output to the antenna.

The performances of the main MMICs are given below.

- Digitally controlled multi-functional MMICs made in GaAs for amplitude/phase conditioning of transmitting and receiving signal. Nominal Tx gain: 11 dB. Nominal Rx gain: 6 dB.
- HPA (GaN) with power switch (GaN) multi-functional MMICs. Saturation output power: 33 dBm. Power Gain: 10 dB.
- DPA (GaAs) with power-switch multi-functional MMICs. Saturation output power: 26 dBm. Power gain: 13 dB.

- LNA (GaAs) with limiter multi-functional MMICs. Nominal gain: 21dB. Nominal NF: 1.5 dB. Limit power: 2 W.

3.2. Circuit Layout and Mechanical Design

The brick-type T/R module is a 2-D package in which MMICs and schematics are located on the same plane. This type of module has the advantages of a simple mechanical structure, a standard development procedure, and a low cost. However, the circuit layout of the brick-type module requires a large area, which contradicts the miniaturized development trend. The tile type with HTCC technology can upgrade the 2-D structure into 3-D structures, which can increase the integration density and decrease the module dimensions and weight. The volume of the tile-type structure is 20–80% of the brick-type's volume. For heat dissipation, the tile-type structure has a shorter thermal path, which results in a higher heat dissipation efficiency.

Therefore, the T/R module designed in this paper is a tile-type structure composed of upper and lower sub-modules that are electrically connected to each other by BGA balls. The lower (HPA-LNA) and the upper (Core-Chip) sub-modules consists of 20 layers. All of the dielectric layers have a fired thickness of 150 μm . The metal fired thickness is 10 μm . A complete overview of the module stack-up is reported in Figure 2, where magenta line represents the RF signal path inside the module. To ensure high electromagnetic compatibility (EMC), both modules first underwent laser welding before stacking. SSMP RF connectors were exclusively used, as they are convenient to assemble and keep the signal's return loss and insertion loss at a low level.

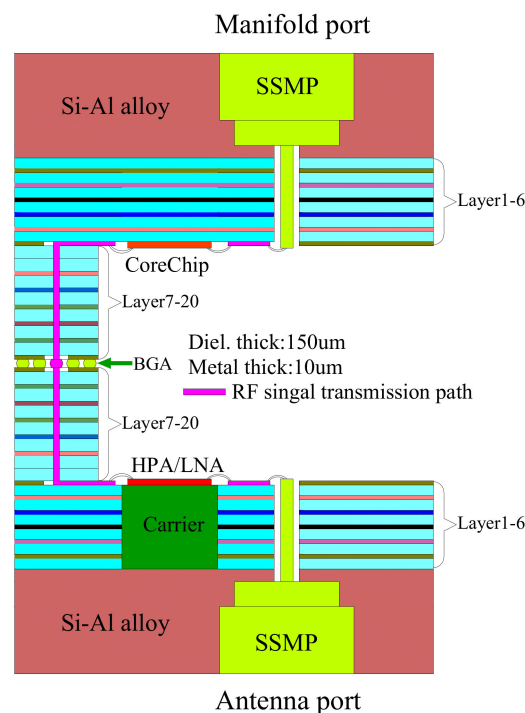


Figure 2. Complete stack-up of the two sub-modules.

The mechanical design of the tile-type T/R module is shown in Figure 3. From the figure, it is clearly seen that the diameter of the BGA balls is 400 μm , and the distance between the BGA balls is 0.7 mm; therefore, they did not need too much space and did not pose a short-circuit risk. Compared to fuzz buttons, BGA balls interconnection has good reliability, low cost, and do not need extra installation fixture due to their simple structure. The circuit loop of BGA balls is shorter than that of fuzz buttons and causes less noise and signal interference.

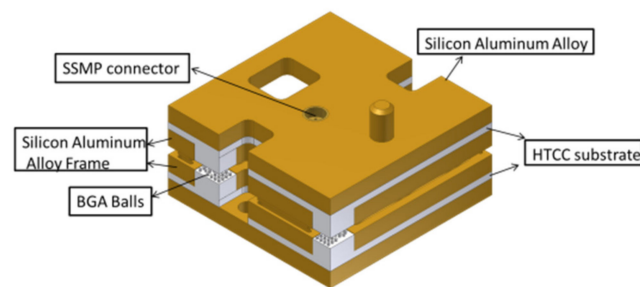
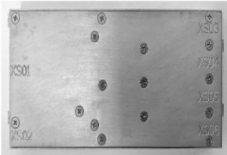
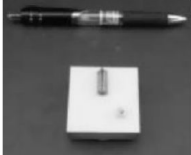
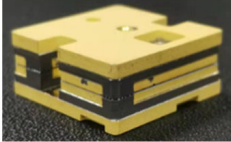


Figure 3. Model of the T/R module.

Table 2 compares the dimensions of our module with those of other T/R modules. With the same channel quantity, the model developed in this paper presents large advantages in size and weight.

Table 2. Comparison of the dimensions of our model with those of other T/R modules.

Module Type	Blade	Tile Type	3-D Tile Type
Physical Photo			
Operating Band	6–18 GHz	2–6 GHz	2–12 GHz
Number of Channels	4	4	4
Dimensions	80 × 37.5 × 10 mm ³	49.8 × 49.8 × 13.5 mm ³	27.8 × 27.8 × 12 mm ³
Weight	60 g	70 g	25 g

3.3. Thermal Design

Each channel of this T/R module has a wideband GaN power amplifier that can output 2 W power. The voltage of the amplifier drain is 28 V, and the peak current of the drain is 500 mA in CW mode, resulting in 12 W heat consumption. If heat consumption cannot dissipate quickly, the amplifier's working temperature will exceed its highest junction temperature, and thus, the amplifier will work abnormally and might burn down.

Considering the above failure situation, the power amplifiers were designed to sinter on Mo–Cu carriers, which have 165 W/m °C thermal conductivity. Mo–Cu carriers directly sinter on the bottom bracket. The material of the bottom bracket is Al–Si 50%, which has 140 W/m °C thermal conductivity. This structure can quickly transfer amplifier heat to the module surface. Based on the physical application environment, the thermal distribution of the total module was simulated. In detail, the heat consumption of the power amplifier was approximately 12 W, and the cooling surface of the module remained at 70 °C. The simulation results in Figure 4 show that the temperature of the amplifier bottom surface was 14.39 °C higher than the temperature of the module bottom surface and much lower than the junction temperature. The power amplifier will work normally in this environment. The thermal expansion coefficients of these amplifiers, carriers, and Al₂O₃ substrate matched each other, which increases the module's reliability.

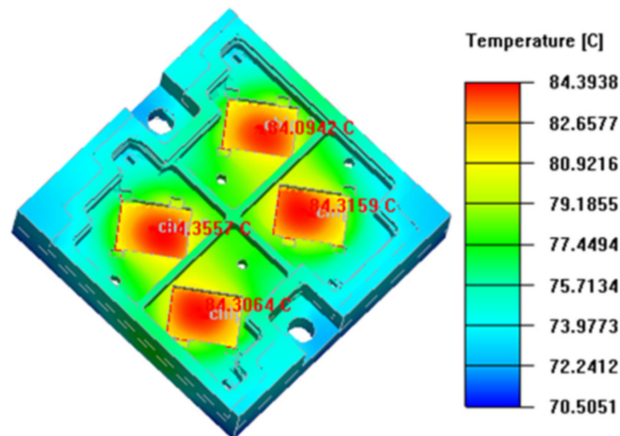


Figure 4. Thermal simulation showing the amplifier working temperature distribution diagram.

4. Key Schematic Design and Circuit Simulation

4.1. BGA Ball Vertical Interconnection

As discussed before, this T/R module is separated into upper and lower sub-modules, which are connected by BGA balls whose diameter is 400 μm . In each sub-module, microstrips and MMICs are electrically connected to each other by bonding gold wires. Therefore, a coaxial-like to microstrip transmission model was built, as shown in Figures 5 and 6.

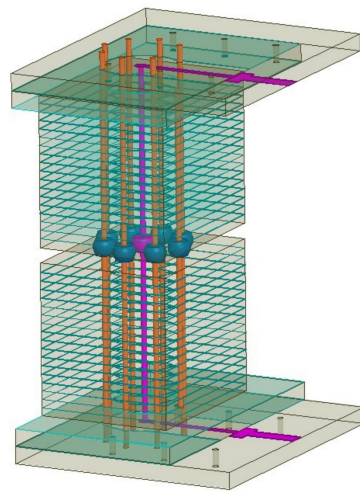


Figure 5. Coaxial-like microstrip simulation model.

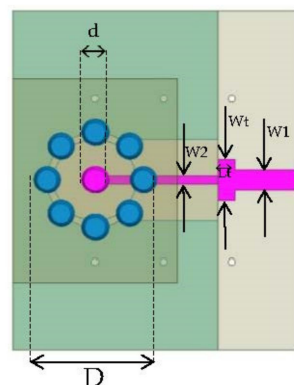


Figure 6. Vertical interconnection matching circuit.

The parameters of the model shown in Figure 6 are presented in Table 3. The impedance of the stripline with W2 wideness and of the microstrip with W1 wideness was 50 ohms. The impedance of the matching line with Wt wideness and Lt length was 42.5 ohms, which could compensate the parasitic inductance generated by the coaxial-like model.

Table 3. Simulation model parameters.

Parameter Name	D	d	W1	W2	Wt	Lt
Value (mm)	1.1	0.4	0.3	0.12	0.42	0.2

In the microwave band, the equivalent series resistance (R_S), series inductance (L_S), and parasitic capacitance (C_{coa}) of a PTH via were determined by the following formulas [10]:

$$R_S = R_{DC} \frac{\pi d^2}{2\pi d \delta} \quad (1)$$

where RDC is the DC resistance, and δ is the skin depth of the PTH via.

$$L_S = \frac{\mu_0 t}{2\pi} \ln(D/d) \quad (2)$$

μ_0 is the permeability of the HTCC substrate.

$$C_{coa} = \frac{\pi \epsilon_r \epsilon_0 t}{\ln(D/d)} \quad (3)$$

In the lumped-parameter formulas above, equivalent series resistance, series inductance, and parasitic capacitance are affected by the operating frequency, height and the radius of the PTH through the via and the outer radius of the circular via array. Based on the formulas above, all parameters were simulated and optimized. The simulation results are shown in Figure 7. For the frequency DC of 20 GHz, S11 was less than -25 dB, and S21 was less than 0.15 dB.

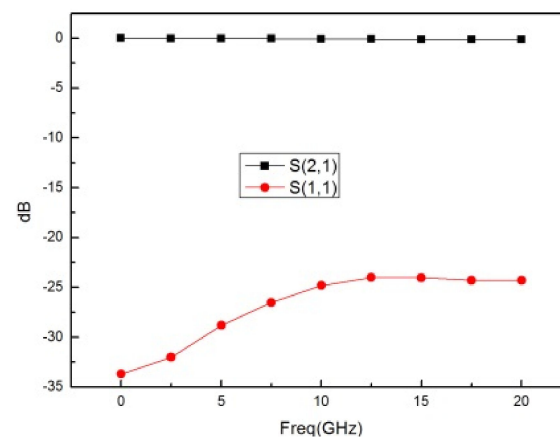


Figure 7. Coaxial-like microstrip simulation result.

4.2. SSMP Vertical Interconnection

SSMP was used as the transmit/receive interface. Because of the tile-type structure, the RF signal had to be transmitted along the SSMP center pin, which vertically passes through the hole in the 1 mm Al_2O_3 substrate. Then, the signal was transferred to the microstrip by bonding wires and transmitted horizontally. Unmatched impedance is generated when the signal is transmitted from the vertical to the horizontal directions. Furthermore, the bonding wires introduce equivalent inductance which will also cause impedance unmatched. The characteristic impedance should be 50 Ω everywhere when the

signal is transmitted in the Al_2O_3 substrate; otherwise, the impedance will be unmatched, which will lead to a high standing wave ratio (SWR) and a high insertion loss. Therefore, for the bonding wires, the length and radius of the gold wires must be limited to decrease the equivalent inductance. Another way is to add stub matches on the transmission lines.

According to the coaxial line principles, coaxial impedance can be calculated as shown below.

$$Z_0 = \frac{60}{\sqrt{\epsilon_r}} \ln \frac{D}{d} \quad (4)$$

where ϵ_r is the dielectric constant. D is the outer radius of the coaxial, and d is the radius of the SSMP center pin. The mixed dielectric materials coaxial model is in Figure 8. The value of d was 0.3 mm; $\varnothing 1$ represents the hole on the HTCC substrate, and its value was 0.5 mm; $\varnothing 2$ represents the via hole diameter in HTCC whose value was 0.12 mm. This value resulted from the minimum via diameter that can be achieved on HTCC. In this case, the dielectric consisted of two materials: air and Al_2O_3 . Therefore, D was difficult to be directly calculated by the formula; the mixed dielectric model was built in HFSS, and the parameter D was swept from 0.46 mm to 0.8 mm. and the simulation results are show in Figure 9.

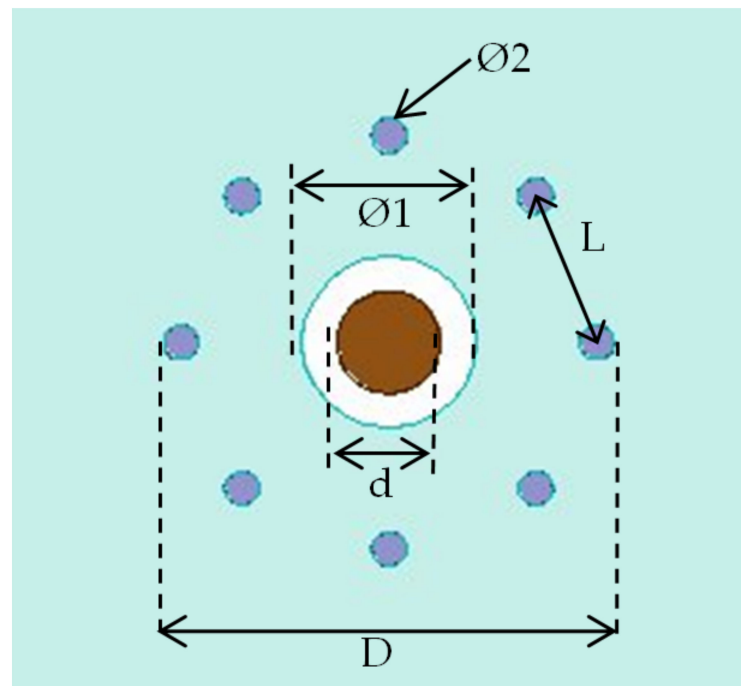


Figure 8. Mixed dielectric materials coaxial model.

From Figure 9, the impedance of the model increased with D increasing. While D was 1 mm, the impedance was closed to 50 ohms. Based on the requirement that the distance between the via holes should be over three times that of the via hole diameter, the value of L was chosen to be 0.38 mm, and the total number of via holes was chosen to be 8. The structure of via holes and SSMP center pin was similar to that of the coaxial. Therefore, this structure was called coaxial-like structure.

The model shown in Figure 8 is not complete. Bonding wires cause inductance in the transmission path, which determines impedance variation; therefore, it was necessary to build a lumped-parameter equivalent model for the gold wires and combine this model with the total model. Figure 10 shows the equivalent circuit of bonding gold wires. R_S and L_S are the equivalent series resistance and inductance, respectively. C_1 is the parasitic capacitance between the wires and the ground.

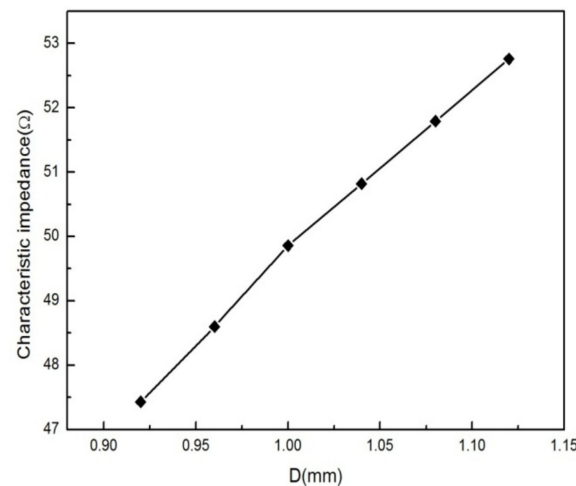


Figure 9. Parameter D sweeping results.

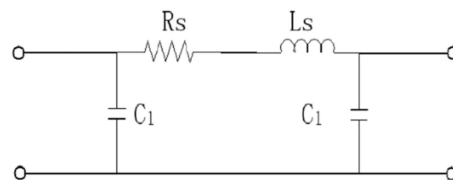


Figure 10. Gold wires lumped-parameter model.

The diameter of a gold wire was $25 \mu\text{m}$, and the capacitance between the wire and the ground was small enough to be ignored. For a cylindrical gold wire whose length is l and whose diameter is d , the expressions for series inductance and resistance are shown below:

$$L_S = \frac{\mu_0 l}{2\pi} \cdot \left[\ln \frac{4l}{d} + \mu_r \frac{\tan(4l/d)}{4} - 1 \right] \quad (5)$$

$$R_S = \begin{cases} \frac{4\sigma l}{\pi d^2} \cos \left[0.041 \left(\frac{d}{d_s} \right)^2 \right], & \frac{d}{d_s} < 3.394 \\ \frac{4\sigma l}{\pi d^2} \cdot \left(\frac{0.025d}{d_s} + 0.02654 \right), & \frac{d}{d_s} \geq 3.394 \end{cases} \quad (6)$$

where μ_0 is the permeability of free space ($\mu_0 = 4\pi \times 10^{-7} \text{ H/m}$). μ_r , ϵ_r , and ρ represent the gold wire's relative permeability, relative conductivity, and resistivity, respectively. In addition, d_s is the skin depth of the gold wire. From the expressions above, the theoretical inductance and resistance can be calculated, which is helpful for optimizing the gold wire model.

Based on the formulas above, a simulation model was built and optimized. The model and results are shown in Figures 11 and 12, respectively. In the frequency range of 2 GHz to 14 GHz, S_{11} was less than -20 dB , and S_{21} was less than 0.2 dB .

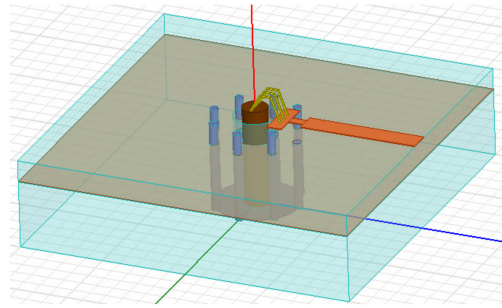


Figure 11. Coaxial with the gold wire model.

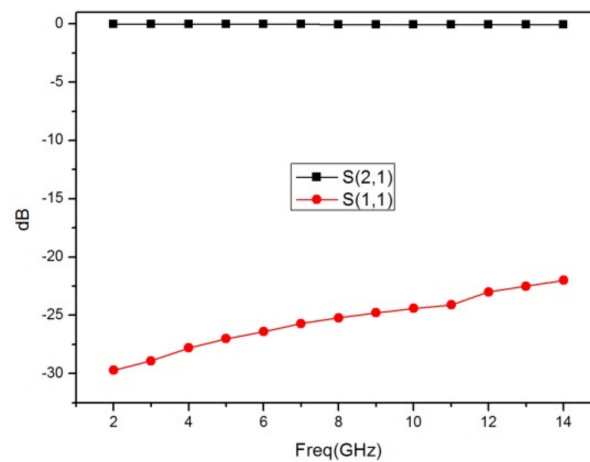


Figure 12. Model simulation results.

5. Module Assembling and Testing

Appropriate temperature levels were set, and an assembly sequence for different components was designed during the module assembly process. Before connecting the upper and lower parts, both parts must be tested to ensure that they can achieve the expected features. Then BGA balls (183 °C) were reballed on the lower module's pads. Next, the upper and lower modules had to be aligned accurately and then reflowed into one module (see Figure 13). As a result, after all these processes, the wideband tile-type T/R module was developed successfully and passed a harsh environment verification test. To perform the test for this tiny module, a customized test fixture was needed.

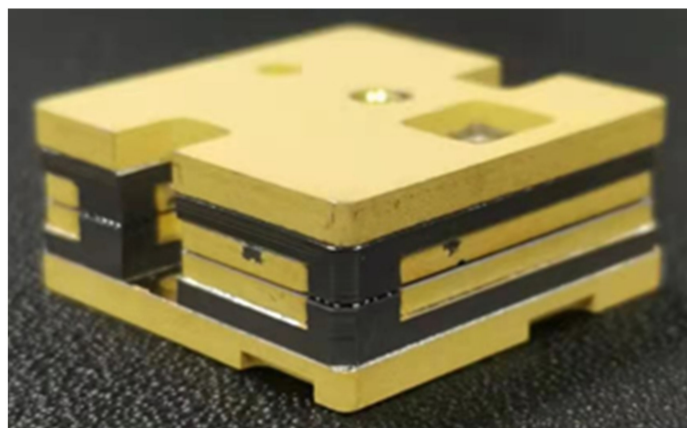


Figure 13. T/R module photo.

Figure 14 describes the test results for this module. In detail, the output power was over 32 dBm, and the in-band flatness was less than 3 dB in the frequency range of 2 GHz–12 GHz. The Tx output power consistency of all four channels was less than 1 dB. When a single channel is working in Tx mode, the peak current is 0.5 A under +28 V and 0.2 A under +5 V, respectively, resulting in an overall 10% power added efficiency.

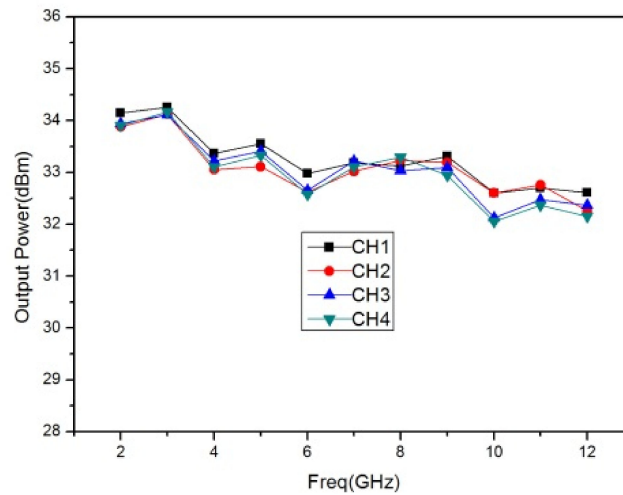


Figure 14. Transmit output power.

Figures 15 and 16 describe the small-signal gain and noise figure results in the receiving mode. In the 2–12 GHz frequency range, the small-signal gain was larger than 15 dB, and the in-band flatness was less than 3.5 dB. The gain consistency of all four channels was less than 1.5 dB. The noise figures of the four channels were less than 5.5 dB. These results satisfy the basic requirements of a phase array radar system for a T/R module.

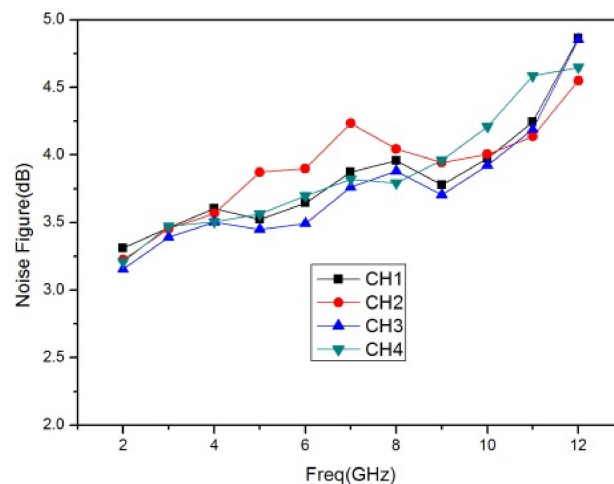


Figure 15. Noise figure.

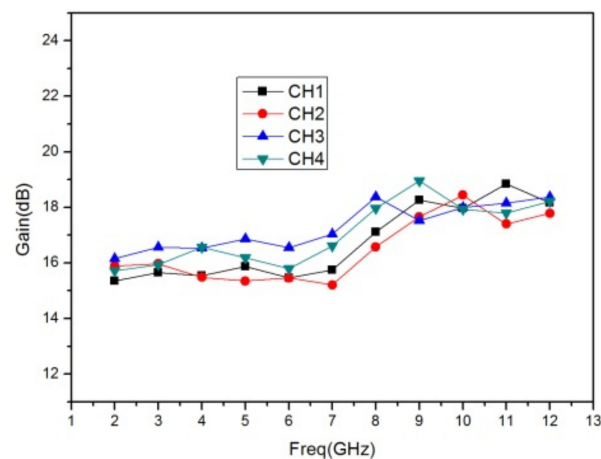


Figure 16. Receive small-signal gain.

6. Conclusions

This paper designed and developed an ultra-wideband, four-channel, tile-type and dual-polarization T/R module according to the application requirements of an active phase array radar system. By applying the BGA interconnection technology to the 3-D package design, we obtained a light and small module, as required. Additionally, by adopting the HTCC multilayer technology and the multifunctional MMICs technology, the diameters further decreased. Despite its small size, the module, maintains high performance, such as high transmit output power, high receive gain, and low receive noise figure in a wide operating frequency range. This module has many advantages and can be widely used in phase array radar systems.

Author Contributions: Writing—original draft preparation, H.S. and Z.L.; writing—review and editing, H.W. and S.Z. All authors have read and agreed to the published version of the manuscript.

Funding: This research received no external funding.

Institutional Review Board Statement: Not applicable.

Informed Consent Statement: Not applicable.

Conflicts of Interest: The authors declare no conflict of interest.

References

- Matevosyan, H.; Poghosyan, A.; Golkar, A. A value-chain analysis for the copernicus earth observation infrastructure evolution: A knowledgebase of users, needs, services, and products. *IEEE Geosci. Remote Sens. Mag.* **2017**, *5*, 19–35. [[CrossRef](#)]
- Bartocci, M.; de Santis, G.; Giolo, G.; Rossi, L.; Gemma, M. 4W TX/RX Multi Chip Module for 6-18GHz Phased Array. In *Gallium Arsenide Applications Symposium, GAAS*; Alma Mater Studiorum-University of Bologna: Bologna, Italy, 2001.
- Alarcón, E.; Sanchez, A.A.; Araguz, C.; Barrot, G.; Bou-Balust, E.; Camps, A.; Cornara, S.; Cote, J.; Peña, A.G.; Lancheros, E.; et al. Design and optimization of a polar satellite mission to complement the copernicus system. *IEEE Access* **2018**, *6*, 34777–34789. [[CrossRef](#)]
- Lacomme, P. New trends in airborne phased array radars. *IEEE Int. Symp.* **2003**, 17–22. [[CrossRef](#)]
- Ma, J.; Sun, W.; Yang, G.; Zhang, D. Hydrological analysis using satellite remote sensing big data and CREST model. *IEEE Access* **2018**, *6*, 9006–9016. [[CrossRef](#)]
- Baccello, D.; D’Antoni, M.; Orobello, B.; Sperduti, E. Miniaturised low cost solid state 4W TXRX common leg for 6–18 GHz phased array. *IEEE MTT-S Int.* **2010**, *1*. [[CrossRef](#)]
- Bian, X.; Shao, Y.; Wang, S.; Tian, W.; Zhang, C. Shallow water depth retrieval from multitemporal sentinel-1 SAR data. *IEEE J. Sel. Top. Appl. Earth Obs. Remote Sens.* **2018**, *11*, 2991–3000. [[CrossRef](#)]
- Schuh, P.; Sledzik, H.; Reber, R.; Fleckenstein, A.; Leberer, R.; Oppermann, M.; Quay, R.; Van Raay, F.; Seelmann-Eggebert, M.; Kiefer, R.; et al. GaN MMIC based T/R-Module Front-End for X-Band Applications. In Proceedings of the 2008 European Microwave Integrated Circuit Conference, Amsterdam, The Netherlands, 27–28 October 2008; pp. 274–277. [[CrossRef](#)]
- Joerg, H.; Pardini, M.; Hajnsek, I.; Papathanassiou, K.P. Sensitivity of SAR tomography to the phenological cycle of agricultural crops at X-, C-, and L-band. *IEEE J. Sel. Top. Appl. Earth Obs. Remote Sens.* **2018**, *11*, 3014–3029. [[CrossRef](#)]

10. Savidis, I.; Friedman, E.G. Closed-form expressions of 3-D via resistance, inductance, and capacitance. *IEEE Trans. Electron Devices* **2009**, *56*, 1873–1881. [[CrossRef](#)]
11. Le, B.T.; Xiao, D.; Mao, Y.; He, D.; Zhang, S.; Sun, X.; Liu, X. Coal exploration based on a multilayer extreme learning machine and satellite images. *IEEE Access* **2018**, *6*, 44328–44339. [[CrossRef](#)]
12. Colangeli, S.; Bentini, A.; Ciccognani, W.; Limiti, E.; Nanni, A. GaN-Based Robust Low-Noise Amplifiers. *IEEE Trans. Electron Devices* **2013**, *60*, 3238–3248. [[CrossRef](#)]
13. Xu, W.; Deng, Y.; Wang, R. Multichannel synthetic aperture radar systems with a planar antenna for future spaceborne microwave remote sensing. *IEEE Aerosp. Electron. Syst. Mag.* **2012**, *27*, 26–30. [[CrossRef](#)]
14. Rieger, R.; Schweizer, B.; Dreher, H.; Reber, R.; Adolph, M.; Feldle, H.-P. Highly integrated cost-effective standard X-band T/R module using LTCC housing concept for automated production. In Proceedings of the IEEE Colloquium on ‘Synthetic Aperture Radar Digest’, London, UK, 29 November 2002; pp. 303–306.
15. Golkar, A.; Cruz, I.L. The federated satellite systems paradigm: Concept and business case evaluation. *Acta Astron.* **2015**, *111*, 230–248. [[CrossRef](#)]
16. Yu, Z.; Xu, Z.; Deng, Y.; Zhang, Z. An Overall LTCC package solution for X-band tile T/R module. *Electromagn. Res. Lett.* **2013**, *38*, 181–192. [[CrossRef](#)]